Journal of Radioanalytical and Nuclear Chemistry (2019) 319:791–803
https://doi.org/10.1007/s10967-018-6376-1

Synthesis of thiol-functionalized hydrotalcite and its application for adsorption of uranium (VI)

Yuanhe Xu[1] · Guojun Ke[1] · Jiang Yin[1] · Weirui Lei[1] · Pengfei Yang[1]

Received: 2 September 2018 / Published online: 12 December 2018

Abstract
The thiol-functional hydrotalcite (Mg/Al-LDO-SH) composite materials were prepared and characterized by EDS, SEM, FT-IR and XRD. The variables influencing the adsorption capacity were investigated. Results show that 3-MPTMS got success in material surface modification. The best optimization condition for adsorption experiment was at time 150 min, pH 3.0, temperature 30 °C, initial uranium (VI) concentration 30 mg L^{-1}, adsorption dosage 10 mg with 99.06% of adsorption efficiency and 1545.32 mg g^{-1} of adsorption capacity. Kinetics data follow the pseudo-second-order model and equilibrium data fit the Freundlich isotherm model very well. Thermodynamic studies show that adsorption process is spontaneous and exothermic.

Keywords Mg/Al-hydrotalcite · Thiol · Adsorption · Uranium (VI) · Functionalize

Introduction

At present, the depletion of fossil fuels has led more and more countries to develop nuclear fission energy to ensure their energy security. As a clean economic energy source with sustainable development, nuclear energy has become an alternative to alleviating the world's energy shortage [1–3]. At the same time, large amounts of uranium are inevitably released into the environment through nuclear fuel cycle activities. Uranium content in wastewater is one of the most difficult pollutants to treat because of its characteristics of non-biodegradability, strong fluidity and persistent pollution [4]. This waste water has long-term effects on human health [5–7]. Therefore, dealing with radioactive nuclear pollution has become a worldwide problem. Currently, methods for removing radioactive elements in water environment include chemical precipitation [8, 9], biological adsorption, solvent extraction [10, 11] and adsorption [12–14]. The adsorption method has been widely applied to the practical wastewater treatment [15–17], because it has the following advantages: high efficiency, low cost, simple processing technology and low secondary pollution [18, 19]. The selection of adsorbent acts directly on the efficiency of the adsorption process [20, 21]. Therefore vast literature is available pertaining to the wide spectra of adsorption materials with stable structure, large specific surface area, active adsorption point and easy modification [22, 23].

Hydrotalcite has a stable structure, open metal sites, large surface and chemically modifiable properties [24, 25], so it is used in the field of adsorption widely [26, 27]. The application of hydrotalcite for adsorption and removal of environmental pollutants has received extensive attention [28–30]. Although hydrotalcite has a good adsorption capacity on anions, it has a small adsorption capacity for uranium [31]. In order to enhance the adsorption capacity of hydrotalcite, we prepared a new material Mg/Al-LDO-SH by Layered Double Oxide (Mg/Al-LDO) modified with 3-TMSPT(-SH). This new material contained active adsorption points and metal chelating sites.

In this study, thiol-functionalized Mg/Al-LDO nanocomposite (Mg/Al-LDO-SH) was synthesised by hydrothermal synthesis method, roasting and grafting of 3-TMSPT. The prepared Mg/Al-LDO-SH is used to adsorb uranium (VI) from Uranium-containing aqueous solutions. The different parameters in the adsorption experiment were investigated and optimized, including pH, doping amount of 3-TMSPT, initial uranium concentration, temperature, adsorbent dosage and contact time. Thermodynamic parameters, kinetics of the process and adsorption isotherms were studied by

✉ Pengfei Yang
ypengfei2008@126.com

[1] School of Chemistry and Chemical Engineering, University of South China, Hengyang 421001, Hunan, China

applying different models. The selectivity and reusability of Mg/Al-LDO-SH were further examined.

Experimental

Materials

$Mg(NO_3)_2{\cdot}6H_2O$, $Al(NO_3)_3{\cdot}9H_2O$, Toluene (C_7H_8), Trimethoxysilylpro-panethiol(3-TMSPT) and $(CO(NH_2)_2$ (Tianjin Tianli Chemical Technology Co., Ltd.); C_7H_8(Toluene), ethanol (CH_3CH_2OH) (Hunan Huihong Reagent Co., Ltd.); CH_3COONa, $ClCH_2COOH$ (Tianjin fuchen Chemical Technology Co., Ltd.); $UO_2(NO_3)_2{\cdot}6H_2O$ (Chushengwei Chemical Technology Co., Ltd.) was used as the 1000 mg/L uranium for uranium standard solution; Deionized water.

X-Max EDS meter(Oxford) was carried out analyzing sample element content; The morphology was characterized using scanning electron microscopy (JSM-7500F SEM analyser); FTIR (Fourier transform infrared spectroscopy) of the samples was analyzed using the Nicolet-460 Fourier transform infrared spectrometer (Thermo Fisher Scientific, USA) in the range of 4000–400 cm^{-1}; T6 Xinrui visible spectrophotometer (Beijing General Analysis Instrument Co., Ltd.) was carried out measure uranium concentration in solution; X-ray diffraction (XRD) was carried out using the Rigaku D/Max IIIB diffractometer.

Synthesis of Mg/Al layered double hydroxide (Mg/Al-LDHs)

Layered double hydroxides (Mg/Al-LDHs) in the carbonate form with molar ratios n $[CO(NH_2)_2]$:n $(Mg^{2+}+Al^{3+}) = 10{:}1$ and n (Mg^{2+}):n $(Al^{3+}) = 2.5{:}1$ were obtained by precipitation from solutions of nitrates Mg and Al by $CO(NH_2)_2$. Solution A was prepared by dissolving $CO(NH_2)_2$ (21.0 g, 0.35 mol) in 50 mL of ultrapure water. Solution B was prepared by dissolving $Mg(NO_3)_2{\cdot}6H_2O$ (6.4 g, 0.025 mol, Mg^{2+}) and $Al(NO_3)_3{\cdot}9H_2O$ (3.75 g, 0.01 mol, Al^{3+}) in 100 mL ultrapure water. The solution A and solution B were simultaneously added to a three-necked flask equipped with a stirrer, and stirring was continued at 60 °C for 30 min. Then the mixed solution was transferred to a Teflon autoclave. Next the Teflon autoclave was placed in an oven and crystallized at 150 °C for 12 h. After the product was crystallized, Mg/Al-LDHs is cooled to room temperature. The solution was centrifuged and washed repeatedly with deionized water five times. The product is dried at 100 °C for 6 h to obtain and named Mg/Al-LDHs [32].

Preparation of Mg/Al layered double oxide (Mg/Al-LDO)

The Mg/Al-LDHs was placed in a muffle furnace and calcined at to 500 °C for 6 h in an air atmosphere. Next the product was removed and cooled to room temperature to obtain Mg/Al-LDO.

Thiol functionalized Mg/Al-LDO (Mg/Al-LDO-SH)

0.5 g Mg/Al-LDO was dispersed in the anhydrous toluene and a certain volume of 3-TMSPT was added to the reaction system. The solution was transferred to the Teflon autoclave after sonicating 30 min. Then mixture solution was placed in an oven at 110 °C for 24 h. After the reaction was completed, the beige solid product was centrifuged, washed with anhydrous toluene and absolute ethanol, respectively. Next, product was placed in a vacuum drying oven and baked at 60 °C for 4 h to obtain Mg/Al-LDO-SH [33]. The synthesis process of Mg/Al-LDHs, Mg/Al-LDO and Mg/Al-LDO-SH are shown in the Fig. 1.

Adsorption experiments

The effects of contact time, dose of 3-TMSPT, pH, temperature, initial uranium (VI) concentration, interfering ions and reusability were examined. In the experiment of measuring the maximum adsorption capacity of the adsorbent, 10 mg of Mg/Al-LDO-SH was first added to the 50 mL flask, then the 20 mL UO_2^{2+} ions solution was added whose concentration was controlled within 5–1000 mg L^{-1}. In order to simulate the treatment of industrial wastewater, the low-concentration adsorption experiments with a uranium concentration of 30 mg L^{-1} (520 mL), pH value 2.0–10.0, and time range of 15–180 min were performed. In addition, the flasks were shaken using mechanical stirring for specified durations at desired temperatures (25–50 °C). The concentration of UO_2^{2+} in aqueous solution was measured by the method of arsenazo III. The pH 2.0 buffer solution of $ClCH_2COOH$/CH_3COONa was prepared. Experimental control group solution contained 0.5 mL arsenazo III [0.05% (w/v)] solution and 0.5 mL deionized water. The experimental group containing 0.5 mL UO_2^{2+} solution, 0.5 mL arsenazo III [0.05% (w/v)] solution and 2.5 mL buffer solution were adjusted to 5.0 mL. The absorbance of the uranium solution was measured using a spectrophotometer at a wavelength of 652.0 nm. In addition, all the above test solutions should be prepared with fresh reagents before each measurement. The adsorption capacity and the adsorption percentage (R) can be calculated using the following Eqs. (1) and (2) respectively.

$$Q = \frac{(C_0 - C_e) \times V}{m} \quad (1)$$

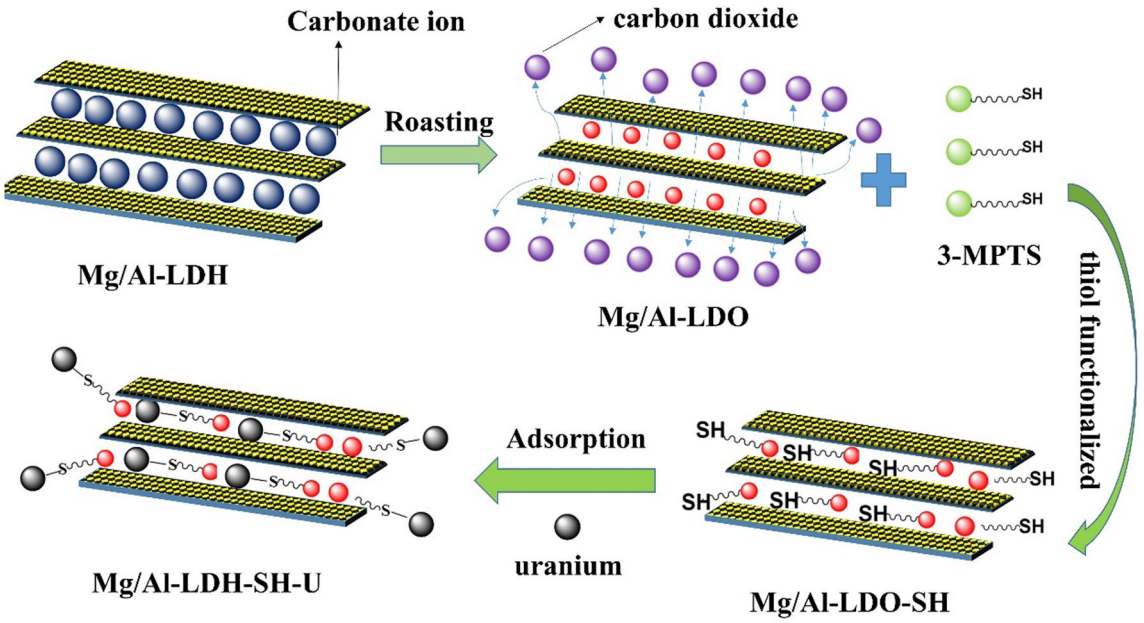

Fig. 1 Synthesis process of Mg/Al-LDHs、Mg/Al-LDO and Mg/Al-LDO-SH

$$R = \frac{(C_0 - C_e)}{C_0} \times 100\% \quad (2)$$

where C_e (mg L^{-1}) is the equilibrium UO_2^{2+} concentration, C_0 (mg L^{-1}) is initial UO_2^{2+} concentration, m (g) is the dosage of Mg/Al-LDO-SH and V (L) is the volume of the UO_2^{2+} experiment solution. Q is the adsorption capacity of Mg/Al-LDO-SH (mg g^{-1}), R is adsorption efficiency of Mg/Al-LDO-SH (%).

In order to study the selective adsorption of uranium (VI) by Mg/Al-LDO-SH in aqueous solution, interfering ion experiments were carried out. Different concentrations (10–80 mg L^{-1}) of interfering ions (such as Zn^{2+}, Fe^{3+}, Cu^{2+}, Ni^{2+}, K^+ and Na^+) were added to the uranium solution (60 mg L^{-1}) and adsorbed for 150 min using the shaker under optimal pH and temperature conditions. After the reaction was completed, the upper layer liquid was centrifuged, and the uranium ion content in the solution was measured using a spectrometric measurement.

In order to investigate the reusability of the Mg/Al-LDO-SH, desorption experiments were carried out. The loaded UO_2^{2+} adsorbent (Mg/Al-LDO-SH-U) after the above adsorption experiment was centrifuged and collected. 100 mL of 0.40 mol L^{-1} NaOH was designated as an eluent for desorption of UO_2^{2+} from Mg/Al-LDO-SH. The Mg/Al-LDO-SH desorbed UO_2^{2+} was centrifuged and collected. Uranium content in the supernatant was measured after each adsorption experiment. And repeated the above adsorption experiment.

Results and discussion

Characterization

The FT-IR spectra of Mg/Al-LDHs, Mg/Al-LDO, Mg/Al-LDO-SH and Mg/Al-LDO-SH-U are shown in Fig. 2. The peaks at 3445.15 is the tensile peaks of O–H over the entire FT-IR spectrum. Compared with the image of Fig. 2a, the typical characteristic peak of M–O–H (Mg, Al)

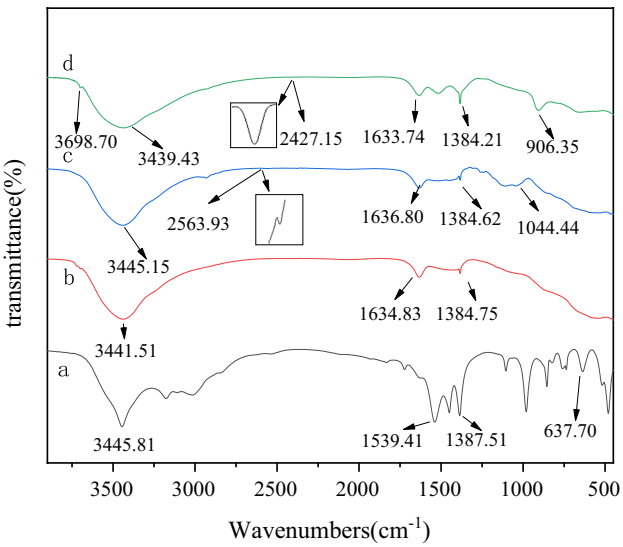

Fig. 2 FT-IR spectra of Mg/Al-LDHs (**a**), Mg/Al-LDO (**b**), Mg/Al-LDO-SH (**c**) and Mg/Al-LDO-SH-U (**d**)

at 637.70 cm^{-1} was disappeared due to the calcination of hydrotalcite in Fig. 2b. Compared with the image of Fig. 2a, b, a typical characteristic peak of -SH at 2563.93 cm^{-1} was observed in Fig. 2c. Combined with EDS spectral analysis, it was proved that thiol has been successfully modified to the surface of Mg/Al-LDO [34]. It can be seen from the comparison between Fig. 2c, d that after uranium ion adsorption, the characteristic peak of -SH at 2563.93 cm^{-1} moved to 2427.15 cm^{-1}, while the characteristic peak of M–O (Mg, Al) at 1044.44 cm^{-1} moved to 906.35 cm^{-1}. The reason is that after the hydrotalcite adsorbs uranium ions, the interlayer structure of the hydrotalcite changes and the characteristic absorption peak shifts. We deduced that the uranium was adsorbed by Mg/Al-LDO-SH successful.

The microscopic structures of Mg/Al-LDHs, Mg/Al-LDO, Mg/Al-LDO-SH and Mg/Al-LDO-SH-U were investigated using SEM with the same magnification. Figure 3a shows that Mg/Al-LDHs has several hundred nanometers in width and several micrometers in length. Product crystal is obviously stick structure. Crystal surface is smooth and the crystal form is relatively intact. Figure 3b shows that Mg/Al-LDO width is narrower than Mg/Al-LDHs, after Mg/Al-LDHs is calcined. Mg/Al-LDO crystals crack and bend but crystal surface is smooth. The product crystal is still intact without obvious damage. Figure 3c shows that Mg/Al-LDO-SH undergoes secondary crystallization when the Mg/Al-LDO is added to the thiol. Although the hydroxides crystals are still rod-like, the crystals have a lot of fractures. Crystal surface is smooth. Figure 3d shows that Mg/Al-LDO-SH-U adsorbs uranium (VI), and the rod structure has not changed. After the material adsorbs uranium solution, the surface is enriched with a large amount of uranium ions to become rough surface and the width of Mg/Al-LDO-SH-U is wider than Mg/Al-LDO-SH. Based on these results, we confirmed that uranium was successfully adsorbed by Mg/Al-LDO-SH.

XRD analysis of Mg/Al-LDHs (a), Mg/Al-LDO (b), Mg/Al-LDO-SH (c) and Mg/Al-LDO-SH-U (d) were shown in Fig. 4. The characteristic diffraction peaks of these samples are stable and the width of these peak are narrow and sharp. In Fig. 4 there is no impurity peak, so the above data indicating that the product has high purity, complete structure and single crystal phase. In Fig. 4a, six characteristic peaks of Mg/Al-LDHs marked by their indices ((003), (006), (012), (015), (018), (110)) were observed for Mg/Al-LDHs [35]. Comparing Fig. 4b, c indicate that they have three common characteristic peaks ((111), (200), (220)). The results show that the Mg/Al-LDO-SH did not change the structure after adding thiol. The SEM image can also prove that the structure of the material was not changed after the thiol was added. In Fig. 4d, there are two characteristic peaks ((131), (220)). The characteristic peaks (131), is compared with the uranium standard card (JCPDS:78-0664). The characteristic peak (131) is the characteristic peak of uranium. As the surface of the material is enriched with a large amount of uranium elements and the outer surface of the adsorbent is covered with a thick layer of uranium ions, the characteristic peaks ((111), (200), (220)) are reduced.

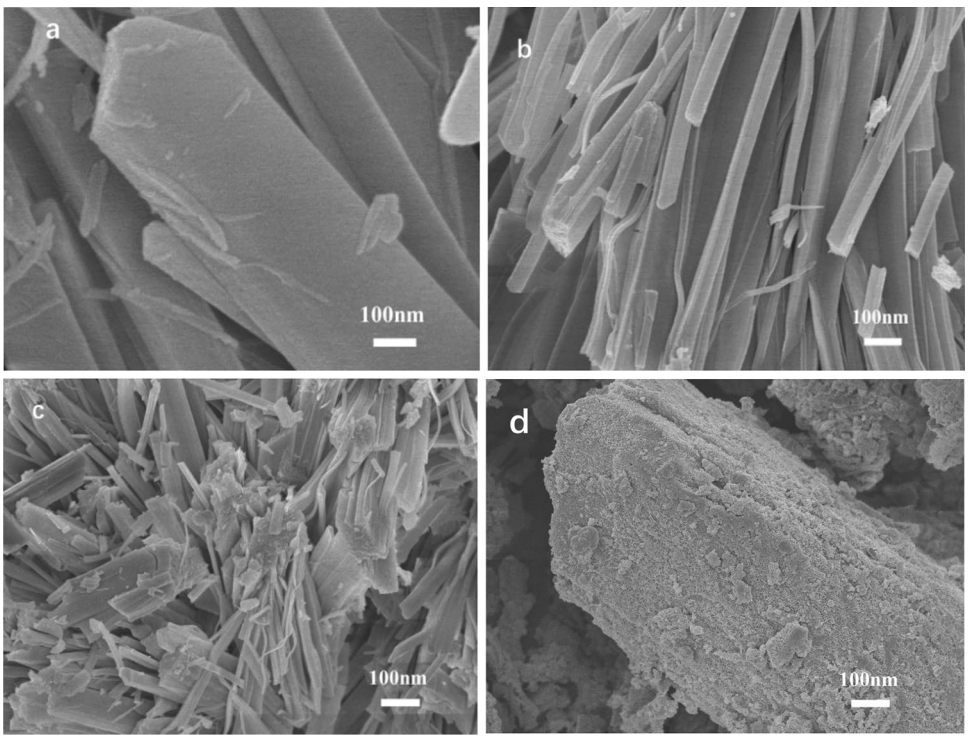

Fig. 3 SEM micrographs of Mg/Al-LDHs (**a**), Mg/Al-LDO (**b**), Mg/Al-LDO-SH (**c**) and Mg/Al-LDO-SH-U (**d**)

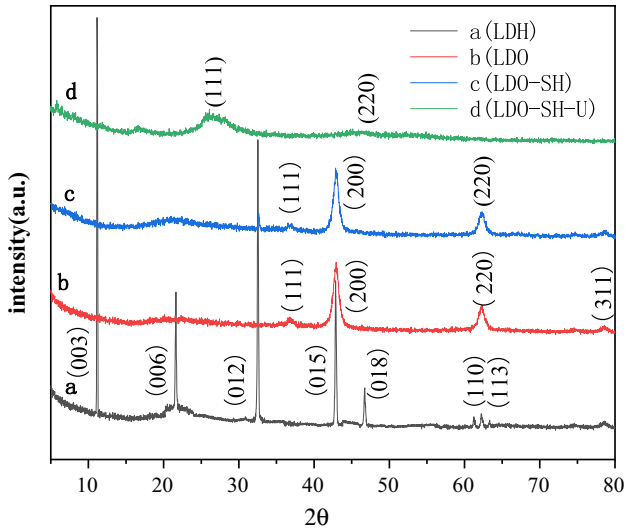

Fig. 4 XRD analysis of Mg/Al-LDHs (**a**), Mg/Al-LDO (**b**), Mg/Al-LDO-SH (**c**) and Mg/Al-LDO-SH-U (**d**)

In Fig. 5a, the EDS spectrum of Mg/Al-LDHs shows only the peaks of aluminum, magnesium and oxygen. As shown in the spectra of Mg/Al-LDO in Fig. 5b, the peak of oxygen presented remarkable reduction, because the carbonate ions are removed after the material is calcined. In Fig. 5c, a strong peak of sulfur appeared. The result illustrated that 3-TMSPT was modified onto the surface of the material successfully. The spectra of Mg/Al-LDO-SH-U in Fig. 5d not only shown peak of sulfur, but also obvious peak of uranium, and the content of sulfur was 66.55 wt%. The results shown that uranium was successfully absorbed by Mg/Al-LDO-SH.

Effect of doping amount of 3-TMSPT

According to the above method, Mg/Al-LDO-SH with 3-TMSPT injection volume of 2, 5, 8 and 12 mL was prepared. Batch experiments were carried out on the condition of temperature 30 °C, initial uranium (VI) concentration 30 mg L^{-1}, pH 3, adsorption dosage 10 mg, volume 520 mL and adsorption time 150 min. The results were presented in Fig. 6. The adsorption amount of UO_2^{2+} by Mg/Al-LDO material is smaller when the injection volume of 3-TMSPT was 0 mL. When the injection volume of 3-TMSPT was 2 mL, the Mg/Al-LDO-SH has the greatest adsorption capacity for UO_2^{2+}. When the injection volume of 3-TMSPT was larger than 2 mL, the adsorption capacity of Mg/Al-LDO-SH decreased as the injection volume of 3-TMSPT increased. The reason is that Hydrotalcite has a lamellar structure. Thiol groups are distributed on the inner and outer surfaces of the plates. When the the load of thiol group is less, the distance between plates is larger, and uranium ions could enter the plate and bind to thiol group. When the load of thiol group is larger, the load of thiol group inside the plate layer is large, thus reducing the distance between the

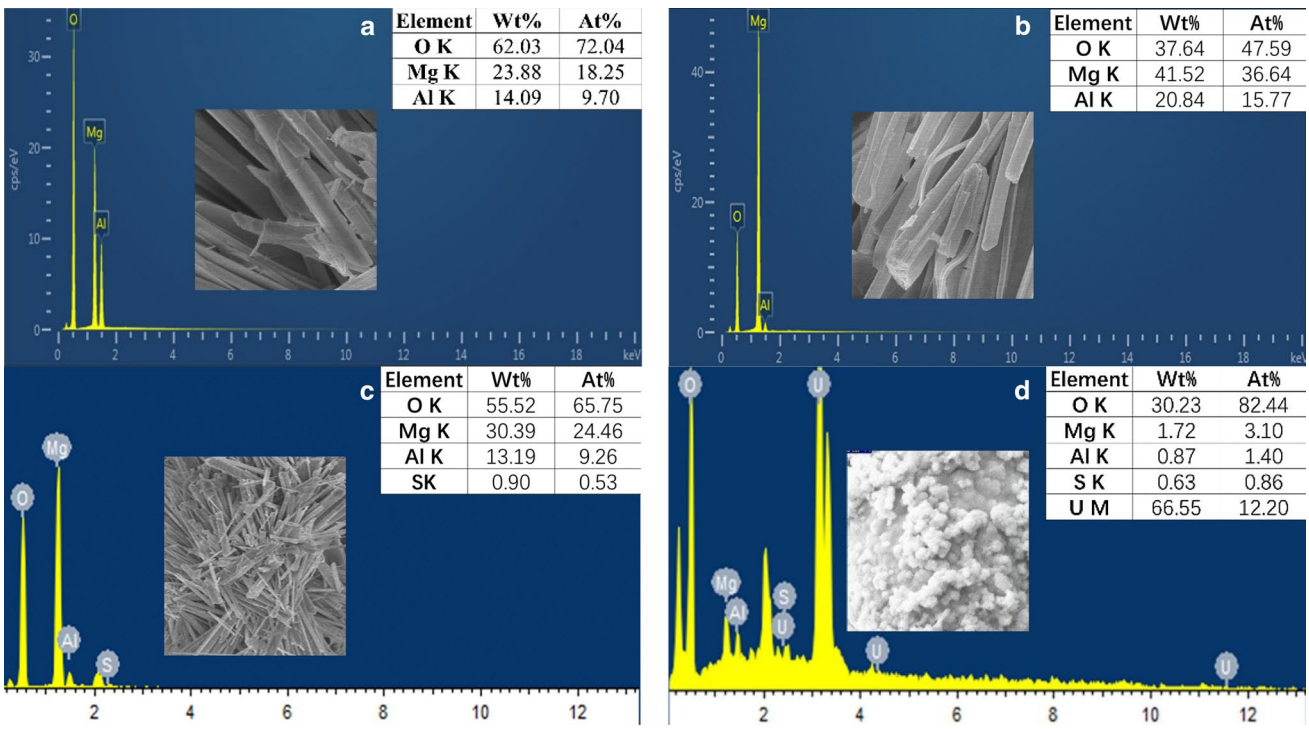

Fig. 5 EDS analysis of Mg/Al-LDHs (**a**), Mg/Al-LDO (**b**), Mg/Al-LDO-SH (**c**) and Mg/Al-LDO-SH-U (**d**)

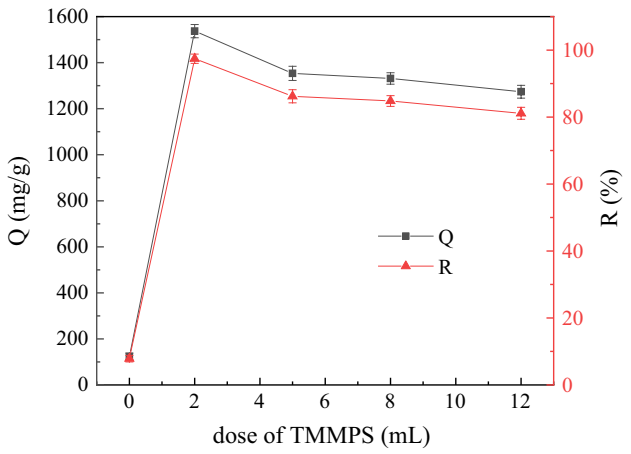

Fig. 6 Influence of doping amount of 3-TMSPT on adsorption performance

plates, uranium ions entering the plate layer and bonding with thiol group is difficult, resulting in a decrease in the adsorption amount of uranium ions by the adsorbent. Therefore, the Mg/Al-LDO-SH prepared with 2 mL of 3-TMSPT is the best adsorbent for uranium. The adsorbent used in the following experiment was a sorbent prepared with 2 mL of thiol.

Effect of adsorbent dosage

Batch experiments were conducted under the condition of temperature 30 °C, pH 3.0, initial concentration 30 mg L^{-1}, volume 520 mL, contact time 150 min and adsorption dosage ranging from 5 to 25 mg. The influence of Mg/Al-LDO-SH dosage on adsorbent efficiency of uranium (VI) was shown in Fig. 7. The adsorption efficiency of the Mg/Al-LDO-SH increases and the adsorption capacity of Mg/Al-LDO-SH decreases as the adsorbent dosage increases between 5 and 10 mg. The reason is that as the dosage of the adsorbent increases, the active adsorption site becomes more and more abundant. When the dosage of Mg/Al-LDO-SH is between 10 and 25 mg, the adsorption efficiency of Mg/Al-LDO-SH is basically the same and the adsorption capacity of Mg/Al-LDO-SH decreases with the increase of adsorbent dosage. The reason is that the dosage of the adsorbent is increased to a certain extent, and the active adsorption site has reached saturation. The results show that 10 mg of adsorbent dosage was considered as the optimum dosage for adsorption of UO_2^{2+}.

Effect of initial concentration

Batch experiments were conducted under the condition of temperature 30 °C, pH 3.0, adsorption dosage 10 mg, volume 20 mL, contact time 150 min, and initial uranium (VI) concentration ranging from 5 to 1000 mg/L. The results were presented in Fig. 8. When the initial concentration of uranium is low, the uranium (VI) in the solution are almost completely absorbed by the Mg/Al-LDO-SH. With the increase of the initial concentration of uranium solution, the active adsorption sites are continuously occupied until the uranium ions in the solution concentration reach 1000 mg/L, and the maximum adsorption capacity of Mg/Al-LDO-SH reaches 1853 mg/g. In order to simulate the treatment of industrial wastewater, the low-concentration adsorption experiment with a uranium concentration of 30 mg/L (520 mL) was performed.

Effect of pH

Batch experiments were conducted under the condition of temperature 30 °C, contact time 150 min, adsorption dosage

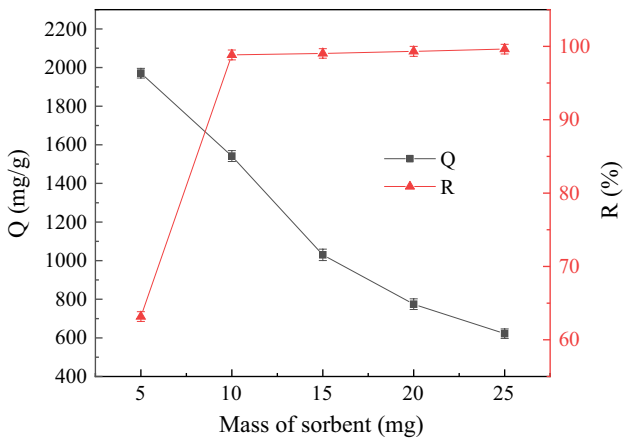

Fig. 7 Effect of adsorbent dosage

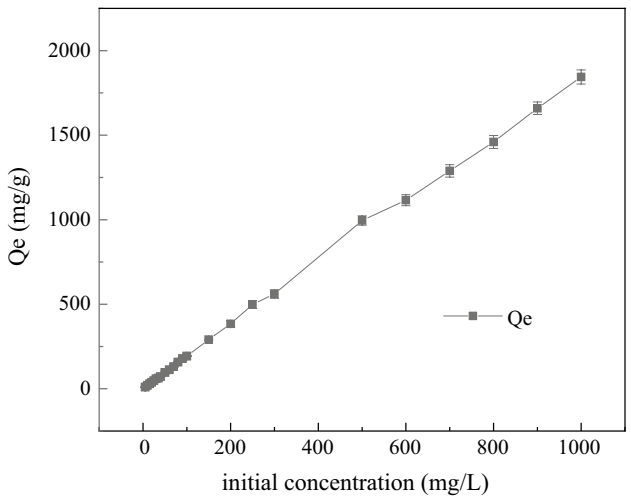

Fig. 8 Effect of initial concentration on adsorption performance

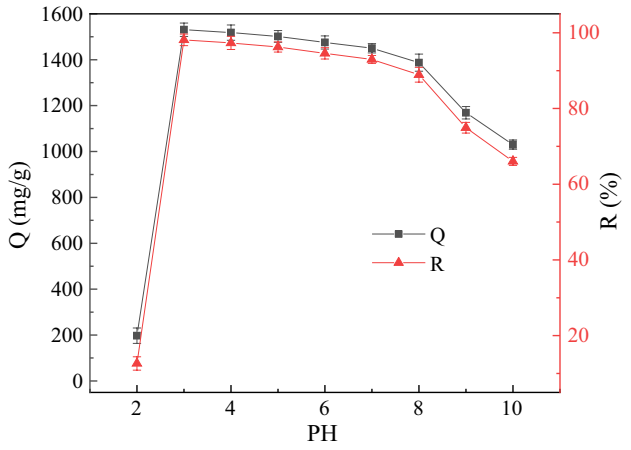

Fig. 9 Influence of pH on adsorption performance

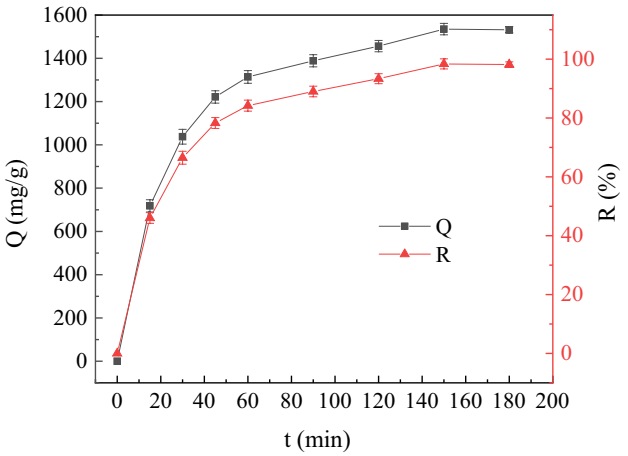

Fig. 10 Influence of contact time

10 mg, initial concentration 30 mg L^{-1}, volume 520 mL and pH value range of 2.0–10.0. The effect of the pH on uranium adsorption was shown in Fig. 9. The adsorption capacity of Mg/Al-LDO-SH increased as the pH of the uranium solution was increased from 2.0 to 3.0. The adsorption capacity of Mg/Al-LDO-SH is basically unchanged as pH of the uranium solution was increased from 3.0 to 8.0. The main reasons are: In the weak acid or weak base environment, the calcined hydroxides has the memory effect. When the structure of Mg/Al-LDO is reconstructed and OH^- is released in water, Mg/Al-LDO-SH increases the basicity of the reaction system and also acts as a buffer. Therefore, in this condition, the ability of Mg/Al-LDO-SH to adsorb uranium ions does not substantially change with the pH value. And then when pH is reduced from 8.0 to 10.0, the adsorption capacity of the adsorbent at higher pH is reduced due to the hydrolysis of UO_2^{2+} into $(UO_2)_2(OH)^{2+}$ and UO_2OH^+ or precipitation [36], resulting in a false impression or adsorption error [37]. The observed lower adsorption capacity of Mg/Al-LDO-SH at pH higher than the optimum values may be due to the precipitation of metal hydroxide and the formation of colloidal [38, 39]. The results show that pH 3.0 was considered to be the optimum pH for Mg/Al-LDO-SH to adsorb UO_2^{2+}.

Effect of adsorption time

In order to study the equilibrium time of Mg/Al-LDO-SH adsorption uranium (VI), batch experiments were conducted under the condition of temperature 30 °C, pH 3.0, adsorption dosage 10 mg, initial concentration 30 mg L^{-1}, volume 520 mL and adsorption time from 30 to 180 min. As shown in Fig. 10, it is evident that the adsorption capacity for uranium (VI) by Mg/Al-LDO-SH increased gradually during the first 30 min, and this might be the thiol with good adsorption property for uranium (VI). With the increase of time, the adsorption rate of uranium ions by Mg/Al-LDO-SH is getting slower and slower. When the time reaches 150 min, the adsorption of uranium by Mg/Al-LDO-SH reaches equilibrium with the maximum adsorption amount of 1545.31 mg g^{-1} and the maximum adsorption efficiency of 99.06%. Therefore, it could be concluded that the adsorption experiments reached an appropriate balance in 150 min with the maximum adsorption amount of 1545.31 mg g^{-1} and the maximum adsorption efficiency of 99.06%.

Effect of temperature and adsorption thermodynamics

Batch experiments were carried out under the conditions of adsorption dosage 10 mg, initial uranium concentration 30 mg L^{-1}, volume 520 mL, time 150 min, pH 3.0 and temperature ranging from 25 to 50 °C. As shown in Fig. 11, in the temperature ranging from 30 to 50 °C, the adsorption capacity of the adsorbent increases with increasing temperature. When the temperature reaches 30 °C, Mg/Al-LDO-SH reaches the maximum adsorption of uranium in aqueous solution. In the range of 30 °C to 50 °C, the adsorption capacity of Mg/Al-LDO-SH for uranium (VI) decreases as the temperature increases. The results show that temperature 30 °C was considered as the optimum temperature for adsorption of UO_2^{2+}.

The relationship between temperature and uranium (VI) adsorption experiments was investigated at 30 °C, 35 °C and 40 °C, respectively. The thermodynamic parameters of the adsorption process were calculated to confirm the thermodynamic feasibility of Mg/Al-LDO-SH and the nature of the adsorption process of Mg/Al-LDO-SH. The observed decrease in both values of Q_m and K_d with elevated temperature for Mg/Al-LDO-SH indicates the exothermic nature of the adsorption process. The values of K_d at different

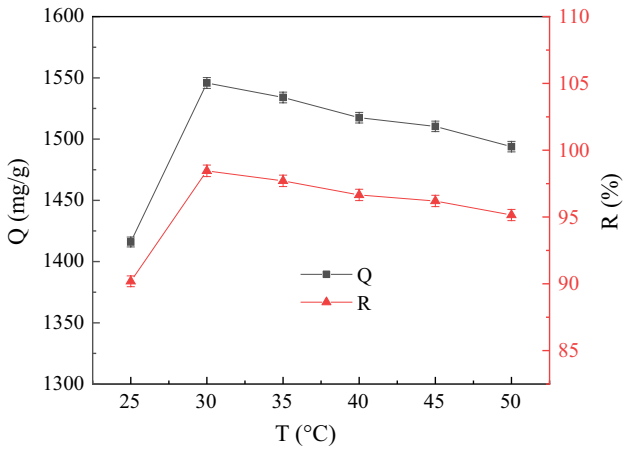

Fig. 11 Influence of temperature

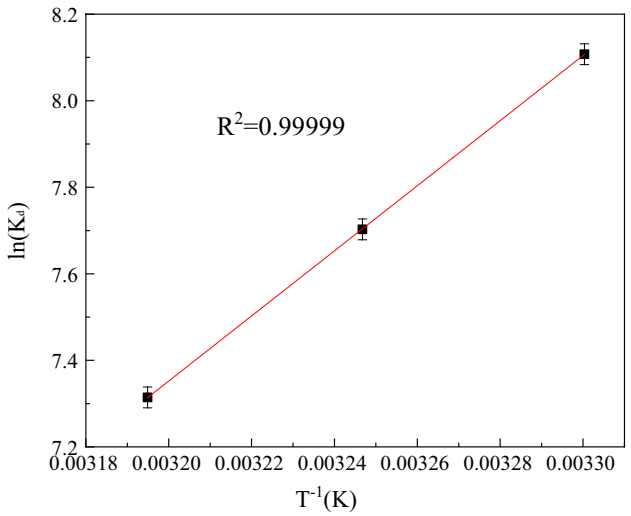

Fig. 12 Plot of In K_d against $1/T$

temperatures were treated according to Van't Hoff equation [40].

$$K_d = \frac{C_0 - C_e}{C_e} \times \frac{V}{m} \tag{3}$$

$$\ln K_d = \frac{\Delta S^0}{\mathrm{R}} - \frac{\Delta H^0}{R \times T} \tag{4}$$

where K_d (mL g^{-1}) is the distribution coefficient, ΔH (kJ mol^{-1}) is enthalpy change, ΔS (J $mol^{-1}K^{-1}$) is entropy change, R (8.314 J $mol^{-1}K^{-1}$) is the universal gas constant, and T (K) is the absolute temperature.

The values of ΔH and ΔS were calculated from Fig. 12 and presented in Table 1. The negative values of ΔH was negative indicates the exothermic nature of the adsorption process. The negative value of ΔS can be explained as the degree of randomness reduced due to the chelation of the uranium (VI) to the active sites of the Mg/Al-LDO-SH to form stable structure [41]. On the other hand, the three-dimensional state of uranium in the solution turns into a two-dimensional existence of the Mg/Al-LDO-SH surface, and its degree of freedom is reduced [42].

Gibbs free energy of adsorption (ΔG) was calculated by the following equation:

$$\Delta G^0 = \Delta H^0 - T \times \Delta S^0 \tag{5}$$

The value of ΔG was negative at different temperatures in Table 3 indicates that the adsorption reaction of the Mg/Al-LDO-SH is spontaneous. On the other hand, the decrease in the negative value of ΔG with increasing temperature means that adsorption of uranium (VI) on Mg/Al-LDO-SH becomes less favorable at higher temperature. The data presented in Table 3 also show at the experimental test temperature, the value of $T\,\Delta S$ is only slightly changed and $|\Delta H| > |T\,\Delta S|$. The above data indicates that the adsorption process is dominated by enthalpy rather than entropic changes.

Adsorption reaction kinetics

In order to study the controlling mechanism of uranium adsorption for Mg/Al-LDO-SH, adsorption experimental data to fit pseudo-first-order and pseudo-second-order, and their rate equations are expressed as follows [43].

$$\text{Pseudo-first-order } \lg(Q_e - Q) = \lg Q_e - \left(\frac{K_1}{2.303}\right)t \tag{6}$$

$$\text{Pseudo-second-order } \frac{t}{Q} = \frac{1}{K_2 Q_e^2} + \frac{t}{Q_e} \tag{7}$$

where Q_t (mg g^{-1}) and Q_e (mg g^{-1}) are the amount of U(VI) adsorbed at time and at equilibrium (min), respectively. K_1 (min^{-1}) and K_2 (g $mg^{-1}h^{-1}$) refer to the rate constant of peudo-first-order and peudo-second-order, respectively.

Table 1 Thermodynamic parameters of UO_2^{2+} adsorption on Mg/Al-LDO-SH

T (K)	ΔG^0 (kJ mol^{-1})	ΔH^0 (kJ mol^{-1})	ΔS^0 (kJ $mol^{-1}K^{-1)}$
303	− 20.40 ± 0.532	− 62.53 ± 0.771	− 138.97 ± 2.500
308	− 19.71 ± 0.545		
313	− 19.01 ± 0.557		

The values of rate constants and correlation coefficients for each model were shown in Figs. 13, 14 and Table 2 after calculated. It was observed from Table 2 that pseudo-second-order ($R^2 = 0.9982$) is superior to the experimental data better than pseudo-first-order ($R^2 = 0.9411$). In addition, the fitting Q_e value based on pseudo-second-order dynamics is closer to the experimental adsorption data (1545.32 mg g^{-1}). The above data indicated that the adsorption experiment could be reasonably approximated by the pseudo-second-order. Therefore, the adsorption process is primarily based on the Chemical adsorption process.

Isotherm modeling

In order to explore the equilibrium concentration and the adsorption capacity of Mg/Al-LDO-SH, The Langmuir and Freundlich isotherms were used to simulate the process of Mg/Al-LDO-SH adsorption of uranium. The two isotherms may be expressed as the following equations, respectively [41]:

$$\text{Langmuir adsorption isotherm: } \frac{1}{Q_e} - \frac{1}{Q_m \times K_a} \times \frac{1}{C_e} + \frac{1}{Q_m} \tag{8}$$

$$\text{Freundlich adsorption isotherm: } \ln Q_e = \ln K_F + \frac{1}{n} \times \ln C_e \tag{9}$$

$$\text{Dubinin–Radushkevich (D–R) isotherm: } \ln Q_e = \ln X_m - \beta\varepsilon^2 \tag{10}$$

$$\varepsilon = RT \ln\left(1 + \frac{1}{C_e}\right) \tag{11}$$

$$E = \frac{1}{(-2\beta)^{\frac{1}{2}}} \tag{12}$$

where Q_e represents the adsorption capacity of Mg/Al-LDO-SH at equilibrium time, C_e is the concentration of solution at equilibrium (mg L^{-1}), Q_m (mg g^{-1}) is the maximal adsorption capacity, K_L (L mg^{-1}) is the Langmuir constant associated with the adsorption energy. K_F is the Freundlich constant. The value of $1/n$ represents the adsorption intensity. X_m (mg g^{-1}) is the maximal adsorption capacity. β represents the activity constant, R (8.314 J $mol^{-1}K^{-1}$) denotes the gas constant and E is the energy.

Figure 15a–c show the adsorption isotherms of uranium adsorption for Mg/Al-LDO-SH. The equilibrium concentration experimental data is modeled according to the Freundlich, D-R isotherm and Langmuir isotherms, and the simulation data was shown in Table 3. According to Fig. 15a–c, compared to the Langmuir isotherm ($R_1^2 = 0.8127$) model and D-R isotherm ($R_3^2 = 0.6503$), the Freundlich isotherm is better described that Mg/Al-LDO-SH adsorbs uranium process and the correlation coefficient is slightly higher ($R_2^2 = 0.9914$). According to Table 3, the values of Q_m and K_L calculated from the intercept and slope of the fitted equation were 1580 and 0.052 L mg^{-1}, respectively. The values of X_m and E are 315 and 2515.6281, respectively. The values of K_F and n are 80.11 and 1.428, respectively. The value of $1 < n$ (1.428) < 10 shown that the adsorption of UO_2^{2+} by Mg/Al-LDO-SH was a multilayer adsorption process. The above analysis show that the Freundlich isotherm model is more suitable for simulating the adsorption of uranium on Mg/Al-LDO-SH.

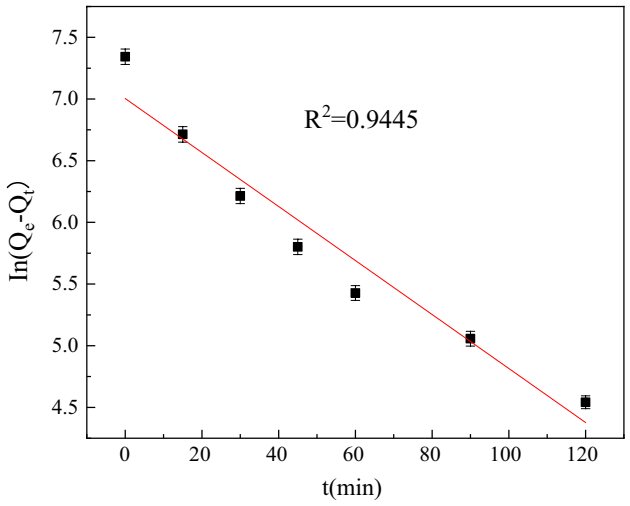

Fig. 13 Pseudo-first-order

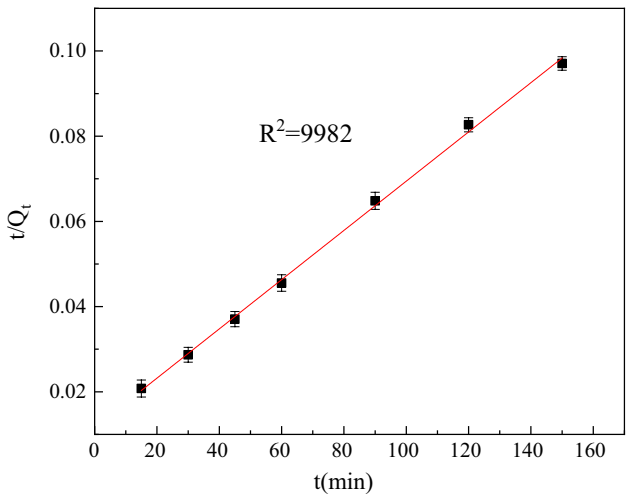

Fig. 14 Pseudo-second-order.

Table 2 Kinetic constants for adsorption of UO_2^{2+} onto Mg/Al-LDO-SH

Pseudo-first-order	Value	Pseudo-second-order	Value
K_1 (min^{-1})	0.02232 ± 0.001	K_2 (mg $g^{-1}min^{-1}$)	0.00002884 ± 0.0000003
Q_e (mg g^{-1})	1117.71 ± 20.02	Q_e (mg g^{-1})	1727.37 ± 18.17
R^2	0.9411	R^2	0.9982
Q_e (exp) (mg g^{-1})	1545.32		

Table 3 Parameters for Langmuir and Freundlich model of UO_2^{2+} onto Mg/Al-LDO-SH

Isotherm parameters	Value
Langmuir isotherm	
Q_m (mg g^{-1})	1580 ± 24.34
K_L (L mol^{-1})	0.052 ± 0.0042
R^2	0.8127
Freundlich isotherm	
K_F (mg g^{-1})/(mg $L^{-1})^{1/n}$	80.38 ± 1.045
n	1.416 ± 0.012
R^2	0.9914
D-R isotherm	
X_m (mg g^{-1})	493.64 ± 1.39
E (kJ mol^{-1})	2342.89 ± 15.51
R^2	0.6166

Effect of interfering ions

A group experiments about the effects of interfering ions we were carried out. Adsorption capacity of Mg/Al-LDO-SH for uranium (VI) in the presence of interfering ions of Na^+, K^+, Fe^{3+}, Cu^{2+}, Zn^{2+}, and Ni^{2+} was shown in Fig. 16. The results show that Na^+, Ni^{2+} and K^+ do not obviously affect the adsorption of UO_2^{2+}. The reason may be that Na^+ (R = 102 pm) and K^+ (R = 132 pm) have too large ionic radii and large steric hindrance, and it is not easy to form a chelate with thiol groups. Fe^{3+}, Cu^{2+} and Zn^{2+} can significantly affect the adsorption of UO_2^{2+}. The reason is that the difference in ionic radii of Fe^{3+} (R = 65 pm), Cu^{2+} (R = 73 pm) and Zn^{2+} (R = 74 pm) and uranium (R = 73 pm) is small, and they have a similar structure. When the interference ion concentration is greater than 15 mg/L, the adsorption effect of Fe^{3+}, Cu^{2+} and Zn^{2+} on UO_2^{2+} increased obviously. In summary, different interfering ions had different influence on adsorption capacity of Mg/Al-LDO-SH for uranium (VI).

Desorption and reusability of the Mg/Al-LDO-SH

The above adsorption experiment steps were repeated to perform a cycle regeneration experiment. 100 mL of 0.40 mol L^{-1} NaOH was designated as an eluent for desorption of UO_2^{2+} from Mg/Al-LDO-SH. Figure 17 shows that the adsorption capacity of the Mg/Al-LDO-SH decreased from 99.06% in the first cycle to 80.13% in the fifth cycle. After five cycles of adsorption and regeneration, the performance of the Mg/Al-LDO-SH did not decrease significantly. The above data indicates Mg/Al-LDO-SH is a kind of repeatable adsorption material after regeneration.

Conclusion

In this paper, a new thiol-functional hydrotalcite (Mg/Al-LDO-SH) composite material was obtained which exhibited high adsorption capacity of Q_{max} = 1853 mg g^{-1} at a high uranium concentration of 1 g/L. And the composite materials were characterized by SEM, FT-IR, EDS and XRD to determine the reliability of the efficient adsorption capacity for uranium. The batch adsorption experiments of Mg/Al-LDO-SH for UO_2^{2+} was optimized at pH 3.0, equilibrium time 150 min, temperature 30 °C and UO_2^{2+} initial concentration 30 mg L^{-1} with 1545.32 mg g^{-1} of adsorption capacity and 99.06% of removal efficiency. The kinetic studies indicate that the adsorption process accords with pseudo second-order dynamic model and is primarily based on the Chemical adsorption process. Equilibrium experiments fit well with the Freundlich adsorption isotherm and show that the adsorption of UO_2^{2+} by Mg/Al-LDO-SH is a multilayer adsorption process. The thermodynamics data indicate that the adsorption process is spontaneous, and exothermic dominated by enthalpy changes. The interfering ions data show that the Mg/Al-LDO-SH has a high selectivity for the adsorption of UO_2^{2+}. The sorbent recovery experimental data indicate that the sorbent has good recycling ability. In addition, the synthesis process of Mg/Al-LDO-SH is simple and the raw materials are cheap. In short, the adsorbent has the characteristics of high adsorption capacity and high selectivity for uranium, which has certain reference value for further research on environmental pollution and wastewater treatment.

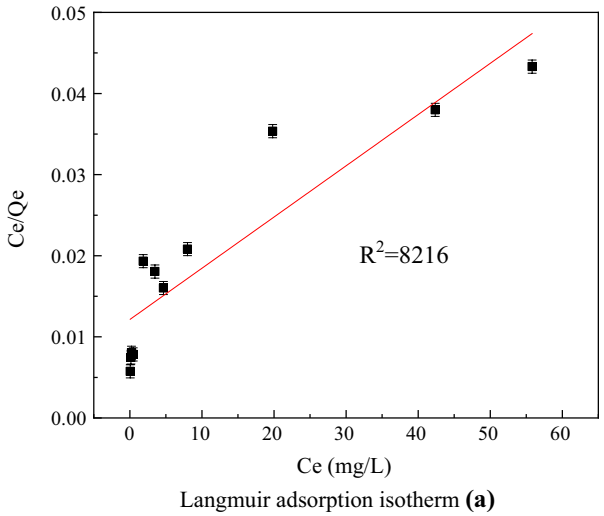

Fig. 15 Linear fitting of Langmuir adsorption isotherm (**a**), Freundlich isotherm (**b**) and Dubinin-Radushkevich isotherm (**c**)

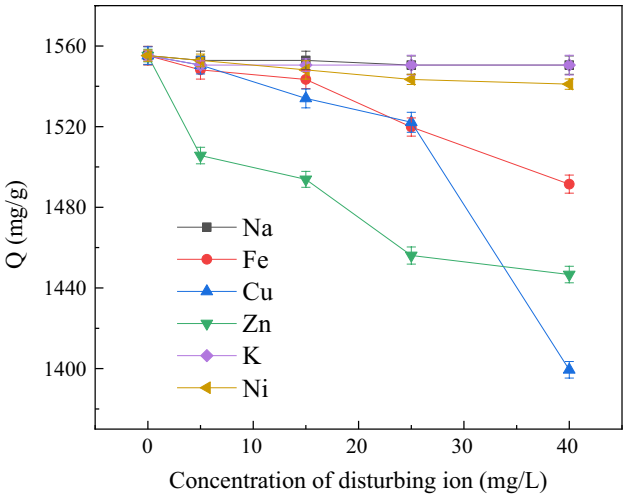

Fig. 16 Effect of interfering ions on Adsorption of Uranium (VI) by Mg/Al-LDO-SH

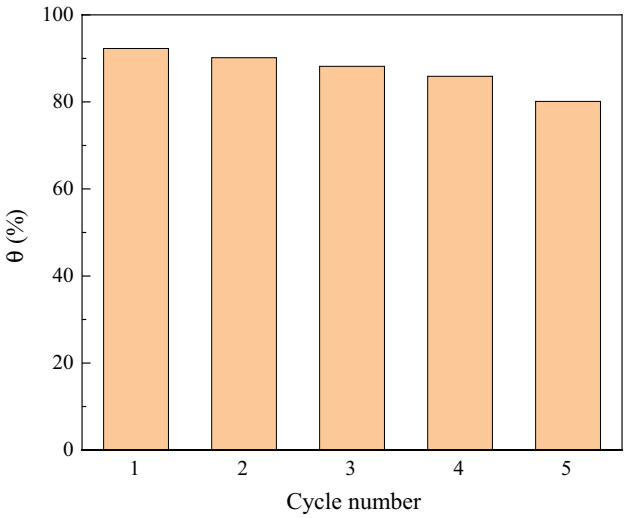

Fig. 17 Influence of cycle times on adsorption performance

Acknowledgements This study was financially supported by the Natural Science Foundation of Hunan Province (2017JJ2231).

Compliance with ethical standards

Conflict of interest All the authors do not have any possible conflicts of interest.

References

1. Craft E, Abu-Qare A, Flaherty M, Garofolo M, Rincavage H, Abou-Donia M (2004) Depleted and natural uranium: chemistry and toxicological effects. J Toxicol Environ Health Part B Crit Rev 7(4):297–317. https://doi.org/10.1080/10937400490452714

2. Duan C, Huo J, Li F, Yang M, Xi H (2018) Ultrafast room-temperature synthesis of hierarchically porous metal–organic frameworks by a versatile cooperative template strategy. J Mater Sci 53:16276–16287
3. Li Z, Chen F, Yuan L, Liu Y, Zhao Y, Chai Z, Shi W (2012) Uranium (VI) adsorption on graphene oxide nanosheets from aqueous solutions. Chem Eng J 210(6):539–546
4. Zhang A, Asakura T, Uchiyama G (2003) The adsorption mechanism of uranium (VI) from seawater on a macroporous fibrous polymeric adsorbent containing amidoxime chelating functional group. React Funct Polym 57(1):67–76
5. Massarin S, Beaudouin R, Zeman F, Floriani M, Gilbin R, Alonzo F, Pery ARR (2011) Biology-based modeling to analyze uranium toxicity data on *Daphnia magna* in a multigeneration study. Environ Sci Technol 45(9):4151
6. Chapman N, Hooper A (2012) The disposal of radioactive wastes underground. Proc Geol Assoc 123(1):46–63
7. Garcã-A-Balboa C, Baselga-Cervera B, Garcã-A-Sanchez A, Igual JM, Lopez-Rodas V, Costas E (2013) Rapid adaptation of microalgae to bodies of water with extreme pollution from uranium mining: an explanation of how mesophilic organisms can rapidly colonise extremely toxic environments. Aquatic Toxicol s 144–145:116–123
8. Kuncham K, Nair S, Durani S, Bose R (2017) Efficient removal of uranium (VI) from aqueous medium using ceria nanocrystals: an adsorption behavioural study. J Radioanal Nucl Chem 313(1):1–12
9. Tripathi S, Roy A, Nair S, Durani S, Bose R (2018) Removal of U(VI) from aqueous solution by adsorption onto synthesized silica and zinc silicate nanotubes: equilibrium and kinetic aspects with application to real samples. Environ Nanotechnol Monit Manag 10
10. Metilda P, Sanghamitra K, Gladis JM, Naidu GRK, Rao TP (2005) Amberlite XAD-4 functionalized with succinic acid for the solid phase extractive preconcentration and separation of uranium (VI). Talanta 65(1):192–200
11. Venkatesan KA, Shyamala KV, Antony MP, Srinivasan TG, Rao PRV (2008) Batch and dynamic extraction of uranium (VI) from nitric acid medium by commercial phosphinic acid resin, Tulsion CH-96. J Radioanal Nucl Chem 275(3):563–570
12. Saini AS, Melo JS (2013) Biosorption of uranium by melanin: kinetic, equilibrium and thermodynamic studies. Bioresour Technol 149(12):155–162
13. Liu N, Wang Y, He C (2016) Tetraphenylimidodiphosphinate as solid phase extractant for preconcentrative separation of thorium from aqueous solution. J Radioanal Nucl Chem 308(2):393–401
14. Lemons B, Khaing H, Ward A, Thakur P (2018) A rapid method for the sequential separation of polonium, plutonium, americium and uranium in drinking water. Appl Radiat Isot 136:10–17
15. Karadağ E, Saraydin D, Güven O (1995) Behaviors of acrylamide/itaconic acid hydrogels in uptake of uranyl ions from aqueous solutions. Sep Sci 30(20):3747–3760
16. Nogami M, Sugiyama Y, Kawasaki T, Harada M, Morita Y, Kikuchi T, Ikeda Y (2010) Adsorptivity of polyvinylpolypyrrolidone for selective separation of U(VI) from nitric acid media. J Radioanal Nucl Chem 283(2):541–546
17. Özeroğlu C, Metin N (2012) Adsorption of uranium ions by crosslinked polyester resin functionalized with acrylic acid from aqueous solutions. J Radioanal Nucl Chem 292(2):923–935
18. Haque E, Lee JE, Jang IT, Hwang YK, Chang JS, Jegal J, Jhung SH (2010) Adsorptive removal of methyl orange from aqueous solution with metal-organic frameworks, porous chromium-benzenedicarboxylates. J Hazard Mater 181(1):535–542
19. Zhang B, Li F, Wu T, Sun D, Li Y (2015) Adsorption of p-nitrophenol from aqueous solutions using nanographite oxide. Colloids Surf A 464:78–88
20. Özeroğlu C, Doğan E, Keçeli G (2011) Investigation of Cs(I) adsorption on densely crosslinked poly(sodium methacrylate) from aqueous solutions. J Radioanal Nucl Chem 289(2):577–586
21. Özeroğlu C, Bilgiç ÖD (2015) Use of the crosslinked copolymer functionalized with acrylic acid for the removal of strontium ions from aqueous solutions. J Radioanal Nucl Chem 305(2):551–565
22. Chen S, Hong J, Yang H, Yang J (2013) Adsorption of uranium (VI) from aqueous solution using a novel graphene oxide-activated carbon felt composite. J Environ Radioact 126(4):253–258
23. Gao MW, Zhu GR, Wang XH, Wang P, Gao CJ (2015) Preparation of short channels SBA-15-PVC membrane and its adsorption properties for removal of uranium (VI). J Radioanal Nucl Chem 304(2):675–682
24. Cheng W, Wan T, Wang X, Wu W, Hu B (2018) Plasma-grafted polyamine/hydrotalcite as high efficient adsorbents for retention of uranium (VI) from aqueous solutions. Chem Eng J 342
25. Yao W, Wang XX, Liang Y, Yu SJ, Gu PC, Sun YB, Xu C, Chen J, Hayat T, Alsaedi A, Wang XK (2018) Synthesis of novel flower-like layered double oxides/carbon dots nanocomposites for U(VI) and Am-241(III) efficient removal: batch and EXAFS studies. Chem Eng J 332:775–786. https://doi.org/10.1016/j.cej.2017.09.011
26. Wang F, Liu Q, Li R, Li Z, Zhang H, Liu L, Wang J (2016) Selective adsorption of uranium (VI) onto prismatic sulfides from aqueous solution. Colloids Surf A 490:215–221
27. Liao Y, Wang M, Chen D (2018) Production of three-dimensional porous polydopamine-functionalized attapulgite/chitosan aerogel for uranium (VI) adsorption. J Radioanal Nucl Chem 316(2):1–13
28. Chitrakar R, Tezuka S, Sonoda A, Sakane K, Ooi K, Hirotsu T (2005) Adsorption of phosphate from seawater on calcined MgMn-layered double hydroxides. J Colloid Interface Sci 290(1):45–51
29. Das J, Patra BS, Baliarsingh N, Parida KM (2006) Adsorption of phosphate by layered double hydroxides in aqueous solutions. Appl Clay Sci 32(3–4):252–260
30. Garciagallastegui A, Iruretagoyena D, Gouvea V, Mokhtar M, Asiri AM, Basahel SN, Althabaiti SA, Alyoubi AO, Chadwick D, Shaffer MSP (2012) Graphene oxide as support for layered double hydroxides: enhancing the CO_2 adsorption capacity. Chem Mater 24(23):4531–4539
31. Tan L, Wang Y, Liu Q, Wang J, Jing X, Liu L, Liu J, Song D (2015) Enhanced adsorption of uranium (VI) using a three-dimensional layered double hydroxide/graphene hybrid material. Chem Eng J 259((Complete)):752–760
32. Guo-Jun KE, Zhang L, Yang PF, Zhao HD, Tan HJ (2017) Controlled synthesis of Mg-Al hydrotalcites with different morphologies and their adsorption performances for chloride ion. Fine Chem
33. Zhang S, Zhang Y, Liu J, Xu Q, Xiao H, Wang X, Xu H, Zhou J (2013) Thiol modified Fe_3O_4@SiO_2 as a robust, high effective, and recycling magnetic sorbent for mercury removal. Chem Eng J 226(24):30–38
34. Lu X, Yin Q, Xin Z, Zhang Z (2010) Powerful adsorption of silver (I) onto thiol-functionalized polysilsesquioxane microspheres. Chem Eng Sci 65(24):6471–6477
35. Fang L, Hou J, Xu C, Wang Y, Li J, Xiao F, Wang D (2018) Enhanced removal of natural organic matters by calcined Mg/Al layered double hydroxide nanocrystalline particles: adsorption, reusability and mechanism studies. Appl Surf Sci 442:45–53
36. Kalin M, Wheeler WN, Meinrath G (2004) The removal of uranium from mining waste water using algal/microbial biomass. J Environ Radioact 78(2):151–177
37. Tong KS, Kassim MJ, Azraa A (2011) Adsorption of copper ion from its aqueous solution by a novel biosorbent *Uncaria gambir*: equilibrium, kinetics, and thermodynamic studies. Chem Eng J 170(1):145–153

38. Atia AA (2005) Studies on the interaction of mercury (II) and uranyl (II) with modified chitosan resins. Hydrometallurgy 80(1–2):13–22
39. Li W, Tao Z (2002) Comparative study on Th(IV) sorption on alumina and silica from aqueous solutions. J Radioanal Nucl Chem 254(1):187–192
40. Fardmousavi O, Faghihian H (2014) Thiol-functionalized hierarchical zeolite nanocomposite for adsorption of Hg^{2+} from aqueous solutions. C R Chim 17(12):1203–1211
41. Zhou L, Shang C, Liu Z, Huang G, Adesina AA (2012) Selective adsorption of uranium (VI) from aqueous solutions using the ion-imprinted magnetic chitosan resins. J Colloid Interface Sci 366(1):165–172
42. Wang Z, Yao Q, Liu P, Li X, Yuan (2011) Kinetics and thermodynamics for acid red 88 adsorption on calcined layered double hydroxides. Acta Chim Sinica 69(5):529–535
43. Li Y, Wang J, Li Z, Liu Q, Liu J, Liu L, Zhang X, Yu J (2013) Ultrasound assisted synthesis of Ca–Al hydrotalcite for U(VI) and Cr(VI) adsorption. Chem Eng J 218(3):295–302